Motility, morphology and phylogeny of the plasmodial worm, *Ceratomyxa vermiformis* n. sp. (Cnidaria: Myxozoa: Myxosporea)

Adriano EA[a,b] *, Okamura B[b]

[a] Departamento de Ciências Biológicas, Universidade Federal de São Paulo (UNIFESP), Diadema, SP, Brazil.

[b] Department of Life Sciences, Natural History Museum, Cromwell Road, London, SW7 5BD UK.

Running head: *A myxozoan plasmodial worm*

***Corresponding author:** Edson A. Adriano, Departamento de Ciências Biológicas, Universidade Federal de São Paulo (UNIFESP), Rua Professor Artur Riedel, 275, Jardim Eldorado, 09972-270 Diadema, SP, Brazil. Email: edapadriano@gmail.com

SUMMARY

The Myxozoa demonstrate extensive morphological simplification and miniaturization relative to their free-living cnidarian ancestors. This is particularly pronounced in the highly derived myxosporeans which develop as plasmodia and pseudoplasmodia. To date, motility in these stages has been linked with membrane deformation (e.g. as pseudopodia and mobile folds). Here we illustrate a motile, elongate plasmodium that undergoes coordinated undulatory locomotion, revealing remarkable convergence to a functional worm at the cellular level. Ultrastructural and confocal analyses of these plasmodia identify a highly differentiated external layer containing an actin-rich network, long tubular mitochondria, abundant microtubules, a secreted glycocalyx layer, and an internal region where sporogony occurs and which contains homogeneously distributed granular/fibrillar material. We consider how some of these features may support motility. We also describe the species based on spore morphology and SSU rDNA sequence data, undertake molecular phylogenetic analysis to place it within an early-diverging clade of the ceratomyxids, and evaluate the resultant implications for classification (validity of the genus *Meglitschia*) and for inferring early host environments (freshwater) of ceratomyxids.

Keywords – Ultrastructure, mitochondrial distribution, vermiform morphology, SSU-rDNA, confocal microscopy, freshwater fish hosts, Amazonia

KEY FINDINGS

- A new myxozoan species with unique worm-like plasmodia was found in gall-bladders of fish from Amazonia
- The elongate plasmodia undergo coordinated undulatory locomotion
- Plasmodia demonstrate convergence to functional worms at the cellular level by a cnidarian
- Ultrastructure, confocal and SEM reveal features that may facilitate motility

INTRODUCTION

Myxozoa are microscopic cnidarians that have undergone extensive morphological simplification and miniaturization as adaptations to parasitism (Okamura et al. 2015). They have complex life cycles involving primarily aquatic vertebrate and invertebrate hosts and are comprised of two classes, the Malacosporea Canning, Curry, Feist, Longshaw & Okamura, 2000 and the Myxosporea Bütschli, 1881. There are some 2,400 described species distributed in 64 genera. The great majority are myxosporeans (Fiala *et al.* 2015a).

Malacosporeans have retained certain primitive features, including muscles in active myxoworm stages produced in some species (e.g. *Buddenbrockia plumatellae*), and epithelia in both myxoworms and the sac-like stages produced in non-motile species. Myxosporeans have lost such tissues and are highly derived. Their trophic stages generally consist of multinucleate plasmodia with many spores or uninucleate pseudoplasmodia that produce one or two spores (Canning and Okamura, 2004).

Motility in myxozoans has been observed in different stages in both malacosporeans and myxosporeans. Some malacosporeans produce myxoworms whose

71 movement is supported by four sets of muscles whose cells are orientated at 12^{o} with
72 respect to the longitudinal axis of the worm (Gruhl and Okamura, 2012). Muscle
73 contraction results in helical swimming. Motility in myxosporeans is achieved at the
74 cellular level via amoeboid movement and 'dancing' (also referred to as twitching) (see
75 Feist *et al.* 2015 for review). The former involves extensions of the cell membrane,
76 often as pseudopodia or filipodia, and there is direct evidence for the involvement of
77 actin (Alama-Bermejo *et al.* 2012). Dancing is observed in blood stages of
78 sphaerosporids and is proposed to be achieved by a mobile fold of the plasmalemma
79 that acts like an undulating membrane (Lom *et al.* 1983).
80 During a survey of fish parasites in rivers of the Amazon Basin, Brazil, we
81 observed a myxosporean with unusually shaped, worm-like plasmodia in the gall-
82 bladder of *Colossoma macropomum* (Cuvier, 1816), a serrassalmid fish of great
83 importance to both the local fish market and Brazilian aquaculture (Goudinho and
84 Carvalho, 1982; MPA, 2012). Here we describe the morphology and motility of this
85 remarkable myxosporean using light, confocal, transmission, and scanning electron
86 microscopy and movements captured by video. We also undertake molecular
87 phylogenetic analysis to determine the relationships of this bizarre species to other
88 myxosporeans. Fine details of morphology along with observed movements enable
89 insights on how convergence to an active worm has been achieved at the cellular level.
90 Morphological and molecular data are also used to describe this new vermiform-like
91 myxosporean species.
92
93 **MATERIAL AND METHODS**
94 ***Collection of material and morphological analysis***

Fifty-three wild *C. macropomum* specimens were collected from the Tapajós, Amazon and Solimões Rivers in Brazil (Table 1). The catches were authorized by the Brazilian Ministry of the Environment (SISBIO n º 44268-4) and fish were transported live to a make-shift field laboratory on the shores of the river, where they were euthanized. The methodology of the present study was approved by the ethics research committee of Federal University of São Paulo (CEUA N 92090802140) in accordance with Brazilian law (Federal Law No. 11794, dated 8 October 2008). All organs and body fluids were examined for myxosporeans and representative material was then collected for morphological and molecular studies (see below). In addition, smears containing free myxospores were air-dried, stained with Giemsa solution and placed in mounting medium on permanent slides. Type specimens were deposited in the collections of the Museum of Zoology "Adão José Cardoso", of State University of Campinas (UNICAMP), Brazil. Morphological and morphometric analyses of myxospores based on Lom and Arthur (1989) and following Gunter *et al*. (2009) (with some modification; see Supplementary File Fig. 1) were performed at the Federal University of São Paulo using a computer equipped with AxioVision 4.1 image capture software coupled to an Axioplan 2 Zeiss microscope.

DNA isolation, sequencing and phylogenetic analysis

Bile from gall bladders infected by worm-like plasmodia was preserved in absolute ethanol for molecular analysis. DNA was extracted using a DNeasy® Blood & Tissue Kit (Qiagen, USA), in accordance with the manufacturer's instructions. The concentration of the DNA was measured using a NanoDrop 2000 spectrophotometer (Thermo Scientific, Wilmington, USA). Polymerase chain reactions (PCRs) were carried out in 25uL reaction volumes using 100 ng of extracted DNA, 5 × Go Taq Flexi

Buffer (Promega), 10 mM dNTP mix, 25 mM $MgCl_2$, 5mM for each primer ERIB1-ERIB10 (Barta *et al.* 1997), and 1x Go Taq G2 Flexi DNA polymerase (Promega). The amplification was performed in an Eppendorf AG 22331 Hamburg Thermocycler (Eppendorf, Hamburg, Germany) using a touchdown PCR method (Korbie and Mattick, 2008), with initial denaturation at 94 °C for 30 s, followed by nine cycles at 94 °C for 30 s, 75 °C (-1 °C/cycle) for 90 s, 72 °C for 45 s, 36 cycles at 94 °C for 30 s, 65 °C for 40 s, 72 °C for 45 s, and then final elongation at 72 °C for 5 min. PCR products were subjected to electrophoresis in 1.0 % agarose gel (BioAmerica, Miami, FL, USA) in TBE buffer (0.045 MTris-borate, 0.001 M EDTA, pH 8.0), stained with ethidium bromide, and then analyzed with a FLA-3000 scanner (Fuji Photo Film, Tokyo, Japan). SSU rDNA was amplified using the primers ERIB1 and ERIB10 (Barta *et al.* 1997), MYXGEN4f (Diamant *et al.* 2004) and a specifically designed primer CERATBr (5'-AGAATTTCACCTCTCGCCATC-3'). The sequencing was performed using the BigDye® Terminator v3.1 cycle sequencing kit (Life Technologies) according to the manufacturer's protocol, adapting the reaction end volume to 5 µl in an ABI 3500 DNA sequencing analyzer (Life Technologies) and using the polymer POP-7 (Life Technologies).

A standard nucleotide-nucleotide Basic Local Alignment Search Tool (BLAST) (blastn) search was conducted (Altschul *et al.* 1997). The sequences of all *Ceratomyxa* species available in GenBank plus *Myxodavisia bulani* KM273030 and *Palliatus indecorus* DQ377712 were aligned by ClustalW (Thompson *et al.* 1997) using the BioEdit program (Hall, 1999). Phylogenetic analysis was conducted using maximum likelihood (ML) in PhyML software (Guindon *et al.* 2010), with NNI search, automatic model selection by SMS (Smart Model Selection), under a GTR+G+I substitution model (with 6 categories), equilibrium frequencies optimized, transition/transversion

ratio estimated, proportion of invariable sites fixed (0.097) and Gamma shape parameter fixed (0.398). To avoid the long branch attraction (LBA) effect (Anderson and Swofford, 2004), Maximum Parsimony (MP) analysis (with complete deletion) was conducted using MEGA7 software (Kumar et al., 2016) on another alignment excluding six long-branching *Ceratomyxa* species. For comparative purposes, ML analysis was also performed using this same dataset, under a GTR+G+I substitution model (with 6 categories), equilibrium frequencies optimized, proportion of invariable sites estimated (0.186) and Gamma shape parameter estimated (0.449). Bootstrap analyses (1000 replicates) were employed to assess the relative robustness of internal branches. The malacosporeans *Tetracapsuloides bryosalmonae* and *Buddenbrockia plumatellae* were used as an outgroup in both phylogenetic analyses.

Electron and confocal microscopy

For transmission electron microscopy, plasmodia were fixed for at least 12 h in 2.5% glutaraldehyde with 0.1 M cacodylate buffer (pH 7.4), washed in the same buffer and post-fixed with osmium tetroxide (OsO_4), all procedures being performed at 4º C. After dehydration in an ascending ethanol series, the samples were embedded in EMbed 812 resin (Electron Microscopy Sciences, Hatfield, PA, USA). Ultrathin sections, double stained with uranyl acetate and lead citrate, were examined using a LEO 906 transmission electron microscope operating at 60 kV. For scanning electron microscopy, infected bile fixed at 10% formalin in 0.1 M PBS was left for 1 h on a polysine pre-treated round coverslip. Coverslips were then washed in the same buffer, dehydrated in ethanol, critical-point-dried, mounted on stubs, covered with metallic gold, and examined in a Zeiss Ultra Plus scanning electron microscope at 5 kV. For confocal analyses, infected bile fixed at 10% formalin in 0.1 M PBS was left for 30 min.

on polysine pre-treated slides. The samples were rinsed three times in PBS and then permeabilized with PBS containing 0.1% Triton X-100 for 1 h. Specimens were then stained with Alexa Fluor® 488 Phalloidin (Invitrogen) at 0.001mg/mL for 4 h and with DAPI (4′,6-Diamidino-2-phenylindole dihydrochloride, Sigma-Aldrich) at 0,004mg/mL for 10 min. The samples were rinsed in PBS and mounted in 90% glycerol, 10% PBS, 0.5% 1,4-diazabicyclo[2.2.2]octane mounting medium. They were examined using a Nikon A1 Confocal Microscope.

Results

Infections in fish

Motile plasmodia of a new myxosporean species were observed in the gall bladders of six of the 53 *C. macropomun* specimens examined. Five of 36 fish examined from the Tapajós River were infected. The single fish examined from the Amazon River was also infected (Table 1). Prevalences of infection were variable and their estimation compromised by low sample sizes, however, data from the Tapajós River suggest that infection prevalences may vary over time (Table 1).

Taxonomic summary and description

Phylum: Cnidaria Verrill, 1865

Class: Myxosporea Bütschli, 1881

Order: Bivalvulida Shulman, 1959

Family: Ceratomyxidae Doflein, 1899

Genus: *Ceratomyxa* Thélohan, 1892

Species: *Ceratomyxa vermiformis* sp. n.

Type host: The fish *Colossoma macropomum Cuvier*, 1818 (Teleostei: Serrasalmidae).

Location in host: Gallbladder (plasmodia with or without mature spores swimming actively in bile).

Type locality: Tapajós River (Municipality of Santarem, PA), Amazon Basin, Brazil.

Type material: Syntypes – air-dried, stained with Giemsa solution and mounted in mounting medium on permanent slides (accession numbers Zuec Myx 54 and 55).

Etymology: The specific name is based on the form and associated movements of the plasmodia, unprecedented observations for myxosporeans.

Movement and morphology

Plasmodia have an elongate form and showed coordinated, worm-like undulations reminiscent of nematode sinusoidal locomotion (Figs. 1 and Videos S1 and S2). The alternating bending movements result in translocation through the bile as can be seen in the Supplementary Material (Video S1).

The plasmodia are characterized by a highly developed cytoplasm that is clearly segregated into an external layer and an internal region. The external layer ranges from around 200 to 600 nm in thickness (Fig. 2A), has an actin-rich cytoskeleton (Fig. 3) and is bounded by an external membrane that is covered by a secreted glycocalyx-like layer (Fig. 2B). Tubular mitochondria, microtubules, rough endoplasmic reticulum and granular material that may represent ribosomes and/or glycogen are abundant in the external layer (Figs. 2 and 4). The elongate mitochondria demonstrate an unusually regular distribution and orientation. Cross-sectional views reveal that the mitochondria are spaced at regular intervals around the periphery of the plasmodia (Fig. 2A) while longitudinal sections demonstrate that their long axis is orientated in parallel with the long axis of the plasmodia (Fig. 4).

The external surface of the plasmodium appears to generally display a series of bulges or ridges that occur as regular transverse bands (Figs. 3 – 6). In certain longitudinal/oblique sections these appear to become highly exaggerated to form a corrugated or peaked surface (Figs. 4 and 5) that extends only partially around the circumference of the plasmodia (Fig 6). SEM suggests this corrugated surface may extend along much of the length of the plasmodia (Fig 6).

The internal region of the plasmodia contains homogeneously distributed granular/fibrillar material. Compared to the external layer, it is less electron-dense and lacks organelles (Figs. 2 and 5). Developing spores are present, but are associated with the external layer at all stages of development (Figs. 2 and 5). Sporogony is asynchronous and plasmodia contain early sporogonic stages and immature and mature myxospores (Figs. 2, 3, 5, 7 and 8). Mature plasmodia containing myxospores had a mean length of 442 µm (SD = 44.9, range =379-520 µm, n = 19) and a mean width of 22.1 µm (SD = 2.6, range = 18-26 µm, n = 19) (Fig. 8). One end of the plasmodium is blunt, while the opposite end is very thin at its extremity (Figs. 3 and 8). Early sporogonic stages are concentrated in the blunt end, specified here as the anterior pole. TEM and confocal microscopy revealed that numerous cells are present in this anterior end (Figs. 2, 3 and 5) and that there is a gradient in maturation of spore developmental stages, with progressively older stages appearing towards the posterior, thin end (the posterior pole) of the plasmodium (Figs. 3, 7 and 8). These observations suggest that the cells in the anterior end represent a growth centre.

The spores are strongly arcuate (Fig. 7 and Fig. S1) with a mean length of 4.5 µm (SD = 0.2, range = 4.2–4.8 µm, n = 28), a mean thickness of 8.4 µm (SD = 0.4, range = 7.9 - 9.3 µm, n = 28) and a posterior angle of 30.2^{o} (SD = 6.6, range = 22 – 43^{o}, n = 18). The two elongated valves resemble appendages that are of unequal size and become

tapered approximately halfway along their lengths. The mean length of the larger valve = 23.7 µm (SD = 0.7, range = 22.1 – 24.3 µm, n = 28) and that of the smaller valve = 21.9 µm (SD = 0.8, range = 20.6 – 23 µm, n = 23). The two polar capsules are spherical and of equal size with a mean diameter of 2.7 µm (SD = 0.1µm, range = 2.5– 2.9 µm, n = 28). The polar filament undergoes 3 to 4 turns oblique to the longitudinal axis of the polar capsule and the binucleated sporoplasm occupies the wider region of the spore (Fig. 7 and Fig. S1).

Phylogenetic analysis

A total of 1.601 bases of SSU rDNA was generated from sequencing of this worm-like myxosporean (GenBank Accession No. KX278420) and molecular phylogenetic analysis performed with ML reveal that it is sister to *Ceratomyxa amazonensis* Mathews, Naldoni, Maia and Adriano, 2016 (Fig. 9). Further molecular phylogenetic analyses performed on a dataset excluding the long-branching *Ceratomyxa* species and using both MP and ML approaches were consistent with this result (Fig. S2). These two species in turn group with *Ceratomyxa leatherjacketi* Fiala, Hlavnickova, Kodadkova, Freeman, Bartošova-Sojkova and Atkinson, 2015 and *Ceratomyxa tunisiensis* Thabet, Mansour, Al Omar & Tlig-Zouari, 2016, forming a lineage with the early diverging *Myxodavisia bulani* Fiala, Hlavnickova, Kodadkova, Freeman, Bartošova-Sojkova and Atkinson, 2015. This *Myxodavisia*/*Ceratomyxa* clade is sister to the remaining *Ceratomyxa* clade (+ *Palliatus indecorus*). The two species of the genus *Ceratonova* Atkinson, Foott and Bartholomew, 2014 cluster together in a separate clade to this large *Ceratomyxa* lineage (Fig. 9 and Fig. S2).

Remarks

The highly arcuate spores of *C. vermiformis* sp. n. with its long and thin valves resembling appendages are similar to those of *Meglitschia mylei* Azevedo, Ribeiro, Clemente, Casal, Lopes, Matos, Al-Quraishy & Matos, 2011, a parasite reported from the serrasalmid fish *Myleus rubripinnis* of the Amazon basin. However, *M. mylei* exhibits a larger number of polar filament turns and smaller sizes of polar capsules and spores than those exhibited by *C. vermiformis* sp. n. In addition, the valves of *C. vermiformis* sp. n. are of unequal sizes whereas they are of a similar size in *M. mylei* (Azevedo et al. 2011) (For detailed comparison see Table S1). Based in these morphological differences we propose the erection of a new species and assign it to the genus *Ceratomyxa*, a decision based on molecular phylogenetic data and an earlier suggestion that the basic spore architecture of *Meglitschia insolita* (Meglitsch, 1960) (first described as *Ceratomyxa insolita*) supports assignment to *Ceratomyxa* (Meglitsch, 1960) as detailed in the discussion section.

DISCUSSION

Fine structure and development in relation to movement

The extraordinary movement displayed by plasmodia of *C. vermiformis* sp. n., as demonstrated in our videos, is associated with particular features that may support or result from motility and movement. These features variously include: a) an actin-rich network distributed throughout the cytoskeleton of the plasmodia; b) the regularly arranged, extremely elongate mitochondria orientated along the longitudinal axis of the worm-like plasmodia, in a peripheral position near the plasmodial membrane; c) a glycocalyx-like layer secreted externally; d) regions of the plasmodial surface that demonstrate regular corrugations; e) microtubules that may function in positioning and contribute to the cytoskeleton (Cooper, 2003; Feist *et al.* 2015); f) segregation to form

294 an electron dense, organelle-rich external layer and an internal region with sporogonic
295 stages but depauperate in organelles. As outlined below, these features provide initial
296 insights on how *C. vermiformis* sp. n. has achieved convergence to a worm-like form at
297 the cellular level.

298 The cuticle-like extracellular secretion and components of the external layer may
299 contribute to hardening or strengthening of the plasmodial wall as is suggested for the
300 external and internal secretions of valve cells in spores (see Gruhl and Okamura, 2015
301 for review). Our combined morphological investigations provide evidence that regions
302 of the wall are highly corrugated (e.g. Figs. 5 and 7). It is possible that the corrugations
303 may result from squeezing and shortening during bending that accentuates the ridged
304 surface of the wall - in which case these would be transient developments. An alternate
305 scenario is that the markedly corrugated regions are permanent features and perhaps
306 serve to increase surface area (e.g. for absorption or to facilitate movement). Further
307 study is required to resolve this issue. The peripheral deployment of microtubules, actin
308 and mitochondria results in a highly consolidated cytoskeleton in the external region.
309 The positioning of the elongate mitochondria around the circumference of the
310 plasmodia may be linked with the distribution of actin, which could influence
311 mitochondrial function (Annesti & Scorrano 2006), for example by shaping, tethering or
312 moving the elongate mitochondria.

313 An additional and notable feature is axial polarity of the plasmodia. The anterior
314 pole is distinguished by a growth centre from which early sporogonic stages show a
315 clear gradient of development to more mature stages distal to this region (see Figs. 3, 7
316 and 8). Gradients in development have also been observed in large histozoic plasmodia
317 where mature spores are located in the periphery (Naldoni et al. 2009; Azevedo et al.
318 2013), but axial polarity in development is absent in amorphous plasmodia. At present it

is unknown whether only one end of the plasmodia of *C. vermiformes* sp. n. consistently leads in the direction of movement. The presence of a polarized primary body axis in a motile myxozoan with a tissue-level of organization has been reported for the malacosporean, *B. plumatellae* (Gruhl and Okamura, 2012).

Amoeboid motility resulting from filipodia has been noted in some *Ceratomyxa* species infecting the gall bladder (Cho *et al.* 2004; Alama-Bermejo *et al.* 2012), and it is proposed that this motility provides a means of avoiding premature release of immature forms with the bile (Alama-Bermejo *et al.* 2012). A similar function may be attributed to the motility of *C. vermiformis* n. sp. Alternatively, swimming may enable the plasmodia to pass through the bile duct into the intestinal tract. In either case, it is striking that very different modes of motility have evolved convergently in cnidarians at the cellular level.

It is notable that certain features associated with bending and contractile movements in protists are also displayed by *C. vermiformis* sp. n., suggesting convergence of form and function at the cellular level. Thus, regularly situated mitochondria are observed to line up in the cortex of ciliates – in this case below a filamentous sheet that is believed to achieve localized bending (Hausman *et al.* 2003). In peritrich ciliates, stalk contraction achieved by the spasmoneme (myoneme) may be antagonized by the extracellular material of the stalk which is proposed to be very elastic (Hausman *et al.* 2003). A similar antagonistic function may be achieved by the extracellular glycocalyx secretion of *C. vermiformis* sp. n. Finally, microtubules in the external layer of *C. vermiformis* sp. n. are likely to serve a cytoskeletal function and might thus function rather like the stiffening rods which are proposed to facilitate coiling in peritrichs (Hausman *et al.* 2003). An alternative or additional explanation for the function of the glycocalyx is protection from the host's digestive enzymes.

344

345 ***A freshwater ancestral environment of ceratomyxids?***

346 Recently Fiala et al. (2015b) identified the *Ceratomyxa* clade as basal to all other
347 marine myxosporean lineages based on molecular phylogenetic analyses using three
348 genes. *C. leatherjacketi* and *M. bulani*, in turn, were revealed to form a basal subclade
349 within *Ceratomyxa*. This basal subclade also now incorporates the newly described *C.*
350 *tunisiensis* and *C. amazonensis* (Mathews *et al.* 2016) and here we show that *C.*
351 *vermiformis* sp. n. groups as sister to *C. amazonensis*. It is notable that fish parasitized
352 by members of the early diverging *Ceratomyxa/Myxodavisia* subclade are associated
353 with freshwater environments. Within this subclade, the early diverging *M. bulani* is a
354 parasite of the amphidromous fish *Megalps cyprinoides* and *C. tunisiensis* has been
355 reported infecting *Caranx rhonchus*, which inhabits brackish-water lagoons and
356 estuaries. *C. amazonensis* and *C. vermiformis* sp. n. parasitize, respectively, *S. discus*
357 and *C. macropomum,* which live exclusively in freshwater environments (Froese and
358 Pauly, 2009). Another parasite of the gall bladder of a serrasalmid fish from the
359 Amazon River (*M. mylei;* Azevedo *et al.* 2011) is also likely to be a member of this
360 clade (see below discussion on *Meglitschia*). Although the bootstrap support in our MP
361 analysis is low, the strong support observed in both ML analyses suggests that infection
362 of hosts associated with freshwater environments may have been primitive for
363 ceratomyxids. This would imply a subsequent extensive radiation of ceratomyxids in
364 hosts inhabiting fully marine environments.

365

366 ***The validity of Genus* Meglitschia**

367 Zao *et al.* (2008) alluded to the general resemblance of *Myxodavisia* and
368 *Ceratomyxa* myxospores and we further point out the similarity of myxospores of *C.*

vermiformis sp. n. to those described for the genus *Meglitschia* Kovaleva, 1988. Kovaleva erected this genus to harbor a species originally described as *Ceratomyxa insolita* (Meglitsch, 1960) (Kovaleva, 1988). In the original description, Meglitsch (1960) argued that although the arcuate spores and large, elongated polar capsules differentiated *C. insolita* (which forms amorphous plasmodia) from other *Ceratomyxa* species described at the time, the basic spore architecture supported assignment to *Ceratomyxa*. Our combined molecular and morphological analyses support Meglitsch's original premise that some *Ceratomyxa* species produce highly arcuate myxospores with elongated and tapered valves. Thus, the minor morphological differences used to create *Meglitschia* appear to be insignificant, suggesting that the genus is not supported. Unfortunately, there are no molecular data available for *Meglitschia* species to help to resolve this issue.

Conclusions

The Myxozoa demonstrate how metazoans have evolved to become endoparasites by miniaturization and morphological simplification as descendants of free-living cnidarian ancestors. The highly derived Myxosporea have taken this to the extreme, having effectively converged with parasitic protists to exploit hosts at the cellular level. Here we show that such miniaturization can nevertheless be accompanied by innovations that may promote coordinated movements as plasmodial worms. However, the basis for such movement at the cellular level in *C. vermiformis* n. sp. remains to be revealed. Whether the remarkable swimming demonstrated by *C. vermiformis* sp. n. is unique, remains unknown as myxozoan diversity is poorly sampled. Further research is likely to reveal new insights on how myxozoans have evolved abilities to move through and to maintain their positions within their host

environments thus illustrating the extraordinary plasticity in lifestyles that can be supported by the cnidarian bauplan.

ACKNOWLEDGEMENTS

We thank Dr. Lincoln Lima Corrêa, Dr. Marcos Tavares-Dias,Marcos Oliveira, Luiz Alfredo da Mata, Eduardo Ferraz de Oliveira, and Raimundo Chicó for help with fieldwork and the fishermen of the communities of Jari do Soccorro, Santarém, Pará, Jarilândia, Macapá and Manacapuru, Amazonas for their local knowledge of fish availability and provision of material for study. We also thank Suellen Zatti for initial sequencing attempts that directed subsequent successful sequencing strategies. We are grateful to Alex Gruhl for advice in the interpretation of fine structure and for comments on our draft manuscript from two referees whose reviews have helped us to improve our manuscript.

FINANCIAL SUPPORT

This study was supported by the São Paulo Research Foundation - FAPESP (Procs. No. 2013/21374-6 - Adriano EA); Adriano EA was supported by a Post-doctoral scholarship from CNPq (Proc. No. 200514/2015-6). Okamura B was supported by the Visiting Researcher Program - FAPESP (Proc. No 2015/19463-6).

REFERENCES

Alama-Bermejo, G., Bron, J.E., Raga, J.A. and Holzer, A.S. (2012). 3D Morphology, ultrastructure and development of *Ceratomyxa puntazzi* stages: First insights into the mechanisms of motility and budding in the Myxozoa. *PLoS ONE* **7**(2), e32679.

Altschul, S.F., Madden, T.L., Schaffer, A.A., Zhang, J.H., Zhang, Z., Miller, W. and Lipman, D.J. (1997). Gapped BLAST and PSIBLAST: a new generation of protein database search programs. *Nucleic Acids Research* **25**, 3389−3402.

Anderson, F.E. and Swofford, D.L. (2004). Should we be worried about long-branch attraction in real data sets? Investigations using metazoan 18S rDNA. *Molecular Phylogenetics and Evolution* **33,** 440–451.

Anest, V. and Scorrano L. (2006). The relationship between mitochondrial shape and function and the cytoskeleton. *Biochimica et Biophysica Acta* **1757,** 692–699.

Atkinson, S. D., Foott, J. S. and Bartholomew, J. L. (2014). Erection of *Ceratonova* n. gen. (Myxosporea: Ceratomyxidae) to encompass freshwater species *C. gasterostea* n. sp. from threespine stickleback (*Gasterosteus aculeatus*) and *C. shasta* n. comb. from salmonid fishes. *Journal of Parasitology* **100**, 640-645.

Azevedo, C., Ribeiro, M., Clemente, S.C.S., Casal, G., Lopes, L., Matos, P., Al-Quraishy, A.S. and Matos, E. (2011). Light and ultrastructural description of *Meglitschia mylei* n. sp. (Myxozoa) from *Myleus rubripinnis* (Teleostei: Serrasalmidae) in the Amazon River system. *Journal of Eukaryotic Microbiology* **58**, 525–528.

Azevedo, C., Clemente, S.C.S., Casal, G., Matos, P., Oliveira, E., Al-Quraishy, A.S. and Matos, E. (2013). Ultrastructure of the plasmodial development of *Myxobolus insignis* (Myxozoa), infecting the amazonian fish *Semaprochilodus insignis* (Prochilodontidae). *Acta Protozoologica* **52,** 91–97.

Barta, J.R., Martin, D.S., Liberator, P.A., Dashkevicz, M., Anderson, J.W., Feighner, S.D., Elbrecht, A., Perkins-Barrow, A., Jenkins, M.C., Danforth, H.D., Ruff, M.D. and Profous-Juchelka H. (1997). Phylogenetic relationships

among eight *Eimeria* species infecting domestic fowl inferred using complete small subunit ribosomal DNA sequences. *Journal of Parasitology* **83**, 262– 271.

Bartošova-Sojkova, P., Hrabcova, M., Peckova, A., Patra, S., Kodadkova, A., Jurajda, P., Tyml, T. and Holzer, A.S. (2014). Hidden diversity and evolutionary trends in malacosporean parasites (Cnidaria: Myxozoa) identified using molecular phylogenetics. *International Journal for Parasitology* **44**, 565–577.

Canning, E.U. and Okamura, B. (2004). Biodiversity and evolution of the Myxozoa. *Advances in Parasitology* **56**, 43–131.

Cho, J.B., Kwon, S.R., Kim, S.K., Nam, Y.K. and Kim, K.H. (2004). Ultrastructure and development of *Ceratomyxa protopsettae* Fujita, 1923 (Myxosporea) in the gallbladder of cultured olive flounder, *Paralichthys olivaceus*. *Acta Protozoologica* **43**, 241–250.

Cooper, G.M. (2003). *The Cell, A Molecular Approach*, 3rd Ed. Sinauer Associates Inc., U.S.

Costa, L.R.F., Barthem, R.B., and Bittencourt, M.M. (2001). A Pesca do tambaqui, *Colossoma macropomum*, com enfoque na área do médio Solimões, Amazonas, Brasil. *Acta Amazonica* **31**, 449-468.

Diamant, A., Whipps, C.M. and Kent, M.L. (2004). A new species of *Sphaeromyxa* (Myxosporea: Sphaeromyxina: Sphaeromyxidae) in devil firefish, *Pterois miles* (Scorpaenidae), from the northern Red Sea: Morphology, ultrastructure, and phylogeny. *Journal of Parasitology* **90**, 1434–1442.

Feist, S.W., Morris, D.J., Alama-Bermejo, G. and Holzer, A.S. (2015). Cellular processes in myxozoans. In *Myxozoan Evolution, Ecology and Development* (ed. Okamura, B., Gruhl, A. and Bartholomew, J.L.), pp. 139-154. Springer International Publishing.

Fiala, I., Bartošová-Sojková, P. and Whipps, C.M. (2015a). Classification and phylogenetics of Myxozoa. In *Myxozoan Evolution, Ecology and Development* (ed. Okamura, B., Gruhl, A. and Bartholomew, J.L.), pp. 85-110. Springer International Publishing.

Fiala, I., Hlavničková, M., Kodádková, A., Freeman, M.A., Bartošová-Sojková, P. and Atkinson, S.D. (2015b). Evolutionary origin of *Ceratonova shasta* and phylogeny of the marine myxosporean lineage. *Molecular Phylogenetics and Evolution* **86**, 75–89.

Froese, R. and Pauly, D. (2009). FishBase. World Wide Web Electronic Publication. Version (03/2009). www.fishbase.org (Accessed on 25/03/2016).

G**oudinho, M. and Carvalho, M.L.** (1982). Life history and management of the tambaqui (*Colossoma macropomum*, Characidae): an important Amazonian food fish. *Revista Brasileira de Zoologia* **1**, 107-133.

Guindon, S., Dufayard, J.F., Lefort, V., Anisimova, M., Hordijk, W. and Gascuel, O. (2010). New algorithms and methods to estimate maximum-likelihood phylogenies: Assessing the performance of PhyML 3.0. *Systematic Biology* **59**, 307-321.

Gunter, N.L., Whipps, C.M. and Adlard, R.D. (2009). *Ceratomyxa* (Myxozoa: Bivalvulida): Robust taxon or genus of convenience? International *Journal for Parasitology* **39**, 1395–1405.

Gruhl, A. and Okamura, B. (2012). Development and myogenesis of the vermiform *Buddenbrockia* (Myxozoa) and implications for cnidarian body plan evolution. *EvoDevo* **3**,10.

Hall, T.A. (1999). BioEdit: A user-friendly biological sequence alignment editor and analysis program for Windows 95/98/NT. *Nucleic Acids Symposium Series* **41**, 95–98.

Hausmann, K., Hülsmann, N. and Radek, R. (2003). *Protistology*. 3rd completely revised edition. E. Schweizerbart´sche Verlagsbuchhandlung (Nägele u. Obermiller): Stuttgart.

Korbie, D.J. and Mattick, J.S. (2008). Touchdown PCR for increased specificity and sensitivity in PCR amplification. *Nature Protocols* **3**, 1452-1456.

Kovaleva, A.A. (1988). Suborder Sphaeromyxina (Myxosporea, Bivalvulida) its structure and place in myxosporidian classification. *Zoologicheskii Zhurnal* **67**, 1616–1620.

Kumar, S., Stecher, G., and Tamura, K. (2016). MEGA7: Molecular Evolutionary Genetics Analysis version 7.0 for bigger datasets. *Molecular Biology and Evolution* **33,** 1870-1874.

Lom, J., Dyková, I. and Pavlásková, M. (1983). "Unidentified" mobile protozoans from the blood of carp and some unsolved problems of myxosporean life cycles. *Journal of Protozoology* **30**, 497-508.

Lom, J. and Arthur, J.R. (1989). A guideline for the preparation of species descriptions in Myxosporea. *Journal Fish Diseases* **12**, 151–156.

Mathews, P.D., Naldoni, J., Maia, A.A.M. and Adriano E.A. (2016). Morphology and small subunit rDNA-based phylogeny of *Ceratomyxa amazonensis* n. sp. parasite of *Symphysodon discus*, an ornamental freshwater fish from Amazon. *Parasitology Research* doi: 10.1007/s00436-016-5173-4.

Meglitsch, P.A. (1960). Some coelozoic Myxosporidia from New Zealand fishes. I. General and family Ceratomyxidae. *Transactions and Proceeding of the Royal Society of New Zealand* **88**, 265–365.

MPA - Ministério da Pesca e Aquicultura (2012). *Boletim estatístico da pesca e aquicultura*. Brasília, Brasil.

Naldoni, J., Arana, S., Maia, A.A.M., Ceccarelli, P.S., Tavares, L.E.R., Borges, F.A., Pozo, C.F. and Adriano E.A. (2009). *Henneguya pseudoplatystoma* n. sp. causing reduction in epithelial area of gills in the farmed pintado, a South American catfish: Histopathology and ultrastructure. *Veterinary Parasitology* **166,** 52–59.

Naldoni, J., Maia, A.A.M., Silva, M.R.M and Adriano E.A. (2014). *Henneguya cuniculator* sp. nov., a parasite of spotted sorubim *Pseudoplatystoma corruscans* in the São Francisco Basin, Brazil. *Diseases of Aquatic Organisms* **107**, 211–221.

Okamura, B., Gruhl, A. and Bartholomew, J.L. (2015). An introduction to myxozoan evolution, ecology and development. In *Myxozoan Evolution, Ecology and Development* (ed. Okamura, B., Gruhl, A. and Bartholomew, J.L.), pp. 1 – 22. Springer International Publishing.

Thompson, J.D., Gibson, T.J., Plewniak, F., Jeanmougin, F. and Higgins, D.G. (1997). The CLUSTAL-X windows interface: flexible strategies for multiple sequence alignment aided by quality analysis tools. *Nucleic Acids Research* **25**, 4876–4882.

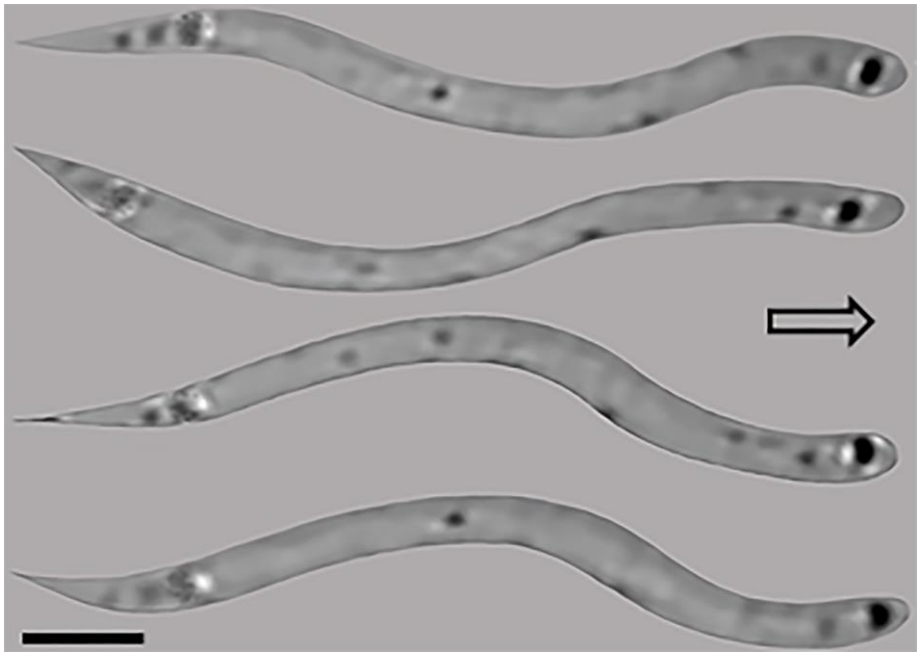

543

544 Figure 1: Images taken from a sequence of video frames showing alternating bending
545 associated with translocation of the worm-like plasmodium of *Ceratomyxa*
546 *vermiformis* sp. n. Images were obtained from video S1. Due to the poor quality of
547 the video (taken during observation in a makeshift field laboratory and using a
548 manually held camera) the outline of the plasmodium has been manually enhanced
549 and we have imposed a uniform background to clarify and distinguish the
550 plasmodium in each frame. Arrow indicates direction of movement. Scale bar = 50
551 µm.
552

553
554
555
556
557
558
559
560
561

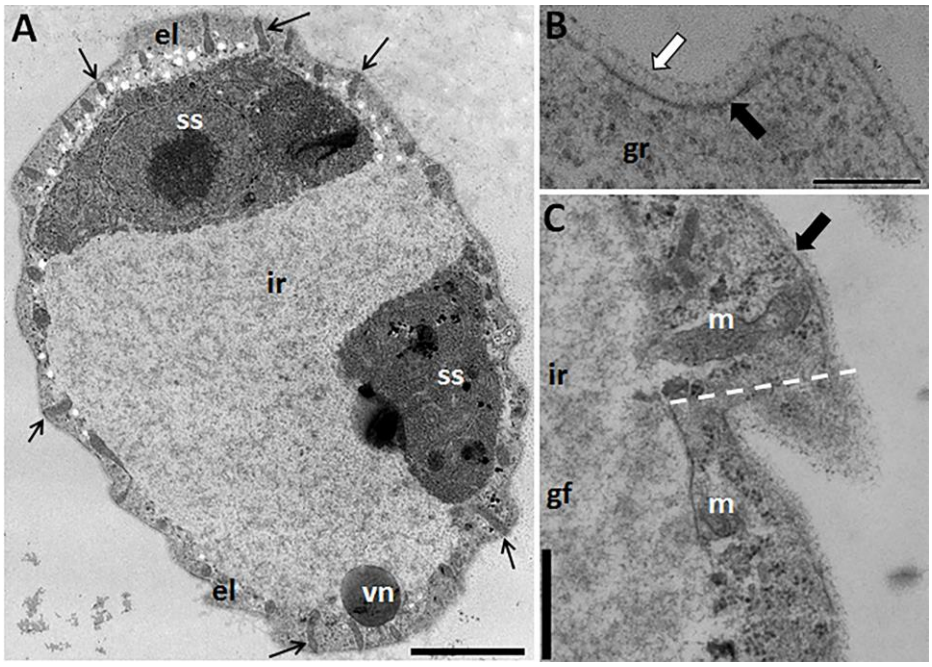

562 Figure 2: Electron micrograph of plasmodia of *Ceratomyxa vermiformi*s sp. n. from the
563 gallbladder of *Colossoma macropomum*. A: transverse section showing external
564 layer (el) with regularly situated mitochondria (black arrows) and early sporogonic
565 stages (ss) developing from the external layer toward the internal region (ir), which

is occupied by granular/fibrilar material. Note a vegetative nucleus (vn). Scale bar = 2 µm. B: amplified region of the external layer showing granular material (gr) and the plasmodial membrane (black arrow) covered by a secreted glycocalyx-like layer (white arrow). Scale bar = 0.25 µm. C: detail of the external layer (dashed line) showing the external membrane (black arrow), a mitochondrion (m) extending from near the cell membrane and extending across the external layer and granular/fibrilar material (gf) occupying the internal region (ir). Scale bar = 0.5 µm.

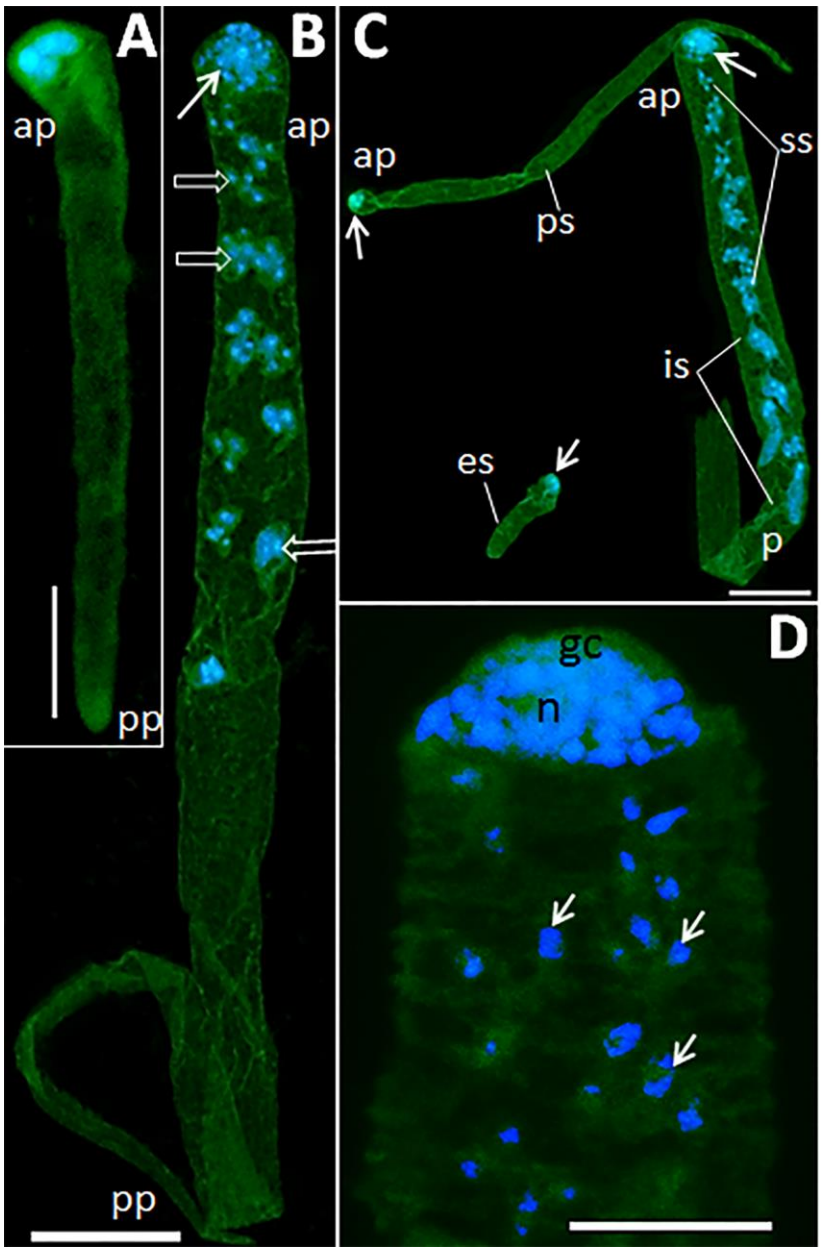

Fig. 3: Confocal laser microscopy photomicrographs showing details of the cytoskeleton and development of plasmodia of *Ceratomyxa vermiformis* sp. n. from the gallbladder of *Colossoma macropomum*. Stains: blue – DAPI; green - Alex Fluor 488 – Phalloidin. A: young plasmodium with nuclei (blue) in the growth centre in the anterior pole (ap). Actin is distributed throughout the cytoskeleton

(green). Scale bar = 10 µm. B: plasmodium showing numerous nuclei (blue) in the growth centre (thin arrow), an actin-rich network throughout the cytoskeleton (green) and developing spores in the interior region of the plasmodium (large arrows). Scale bar = 25 µm. C: plasmodia in different developmental stages including an early developmental stage (es), a later but still pre-sporogonic stage (ps) and a more mature plasmodium (p) with internal stages at early stages of spore development (ed) and immature spores (is). Scale bar = 25 µm. D: details of the anterior pole of a plasmodium showing numerous nuclei (n) in the growth centre (gc) and nuclei of early sporogonic stages (thin arrows) below. Scale bar = 10 µm. Posterior pole = pp.

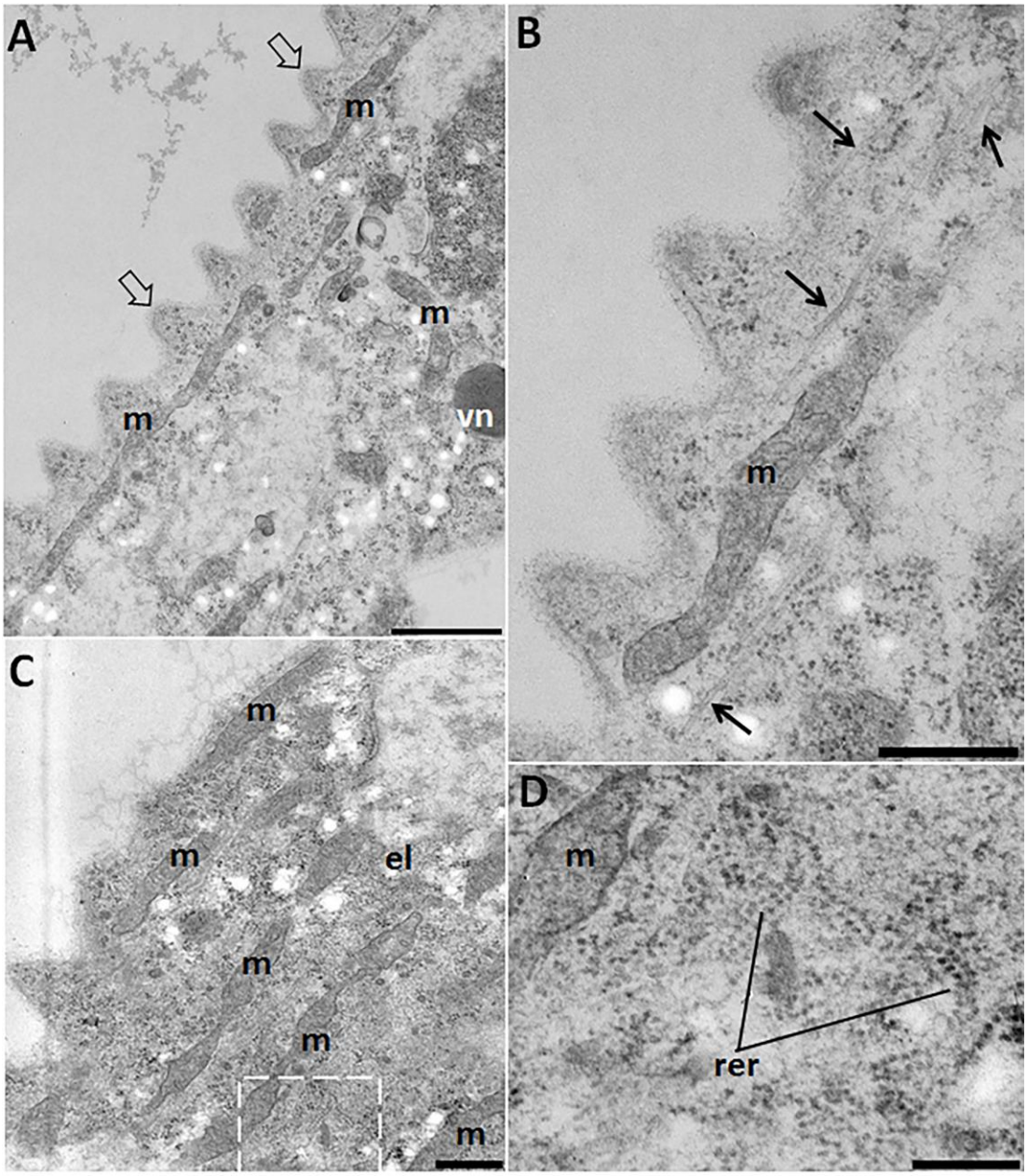

Figure 4: Electron micrographs of plasmodia of *Ceratomyxa vermiformis* sp. n. from gallbladder of *Colossoma macropomum* in longitudinal section. A: showing corrugated surface (arrows), long tubular mitochondria and part of a vegetative

nucleus (vn) and of a young sporogonic stage Scale bar = 1 µm. B: amplified micrograph of the area of the upper right corner of Fig. A showing longitudinal sections of microtubules (arrows) and a long tubular mitochondrion (M). Scale bar = 1 µm. C: oblique view showing the regular organization of the mitochondria (m) in the external layer (el). Scale bar = 0.5 µm. D: detail of marked area of Fig. C showing fragment of a mitochondrion (m) and rough endoplasmic reticulum (rer). Scale bar = 0.25 µm.

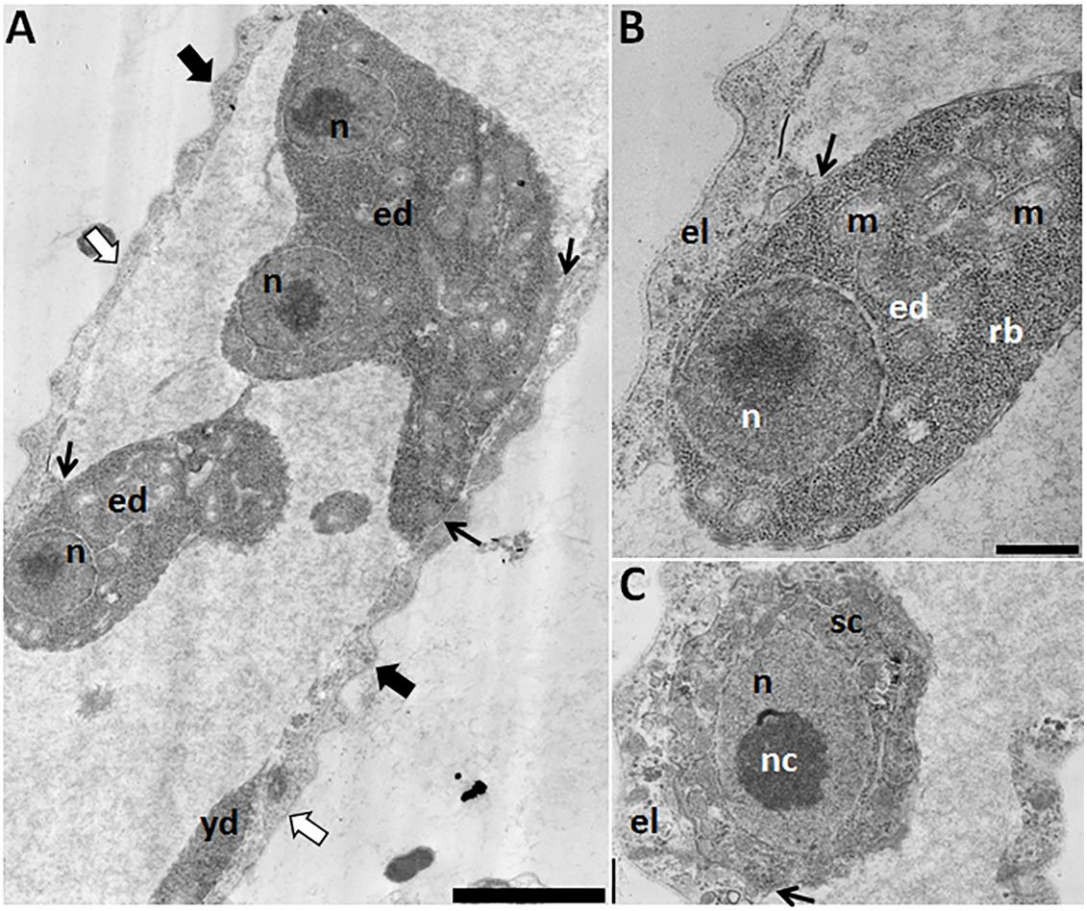

Figure 5: Electron micrograph of plasmodia of *Ceratomyxa vermiformis* sp. n. from gallbladder of *Colossoma macropomum*. A: longitudinal section showing the early developmental sporogonic forms (ed) associated with the external layer (thin black arrows). Note regions of the plasmodial surface with (large black arrows) and without (large white arrows) corrugations. Scale bar = 2 µm. B: amplified region of Fig. 5A showing early developmental spore (ed) associated with the external layer (el) (thin black arrows); m: mitochondria; n: nucleus. C: Transverse section showing a sporogonic cell (sc) developing in proximity to the external layer (el) (thin arrow); n: nucleus, nc: nucleolus. Scale bar: B and C = 0.5 µm.

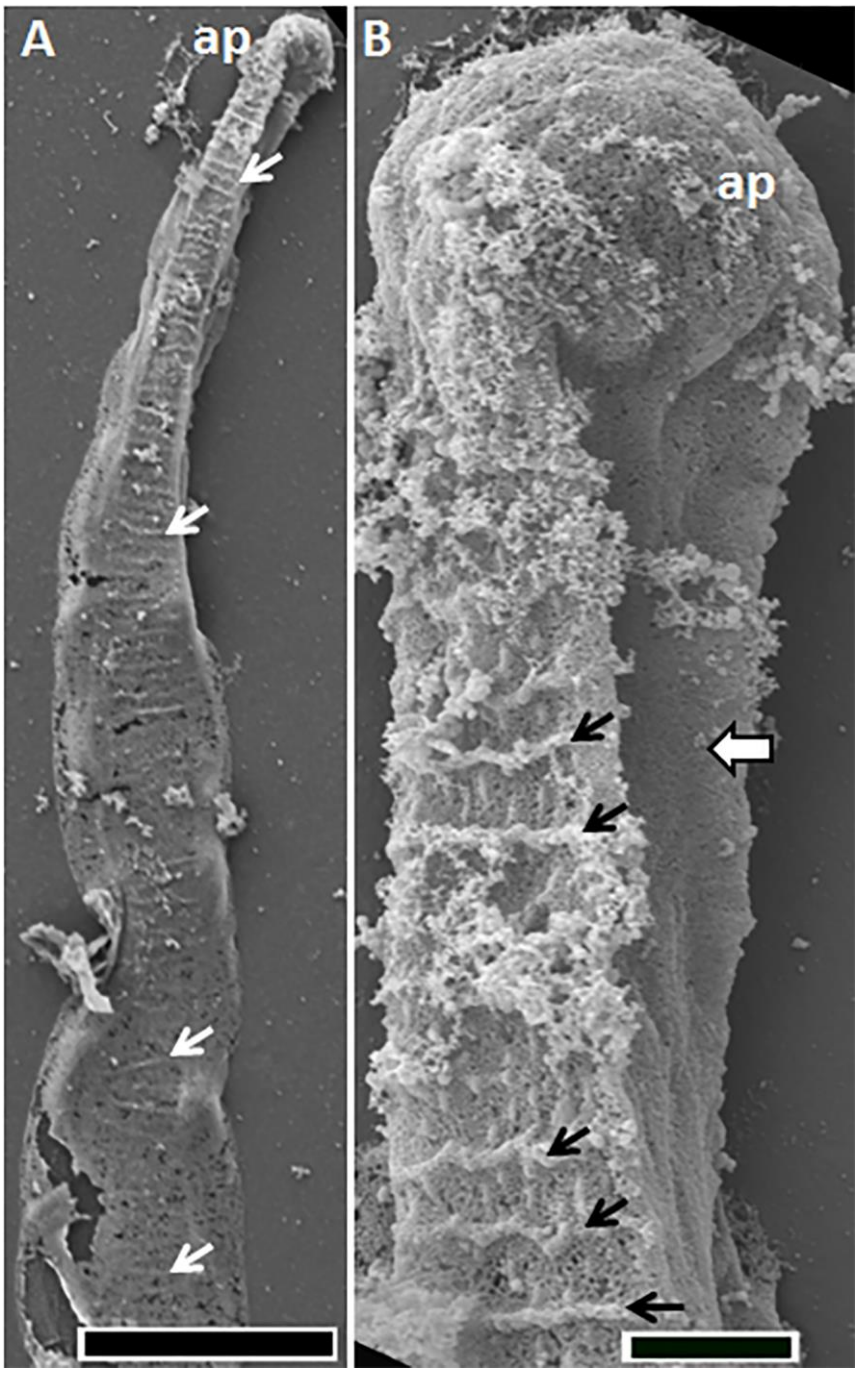

Fig. 6: Scanning electron microscopy of anterior region of plasmodia of *Ceratomyxa vermiformis* sp. n. from the gallbladder of *Colossoma macropomum*. A: showing presence of corrugations (arrows) extending a considerable distance posterior from the anterior pole (ap). Despite damage to the specimen the corrugations can be seen to become less regular in posterior direction and eventually disappear (not shown). Scale bar = 20 µm. B: more detailed view demonstrating the presence (thin arrows) and absence of corrugations on different facets of the plasmodium (large arrow). Scale bar = 2 µm.

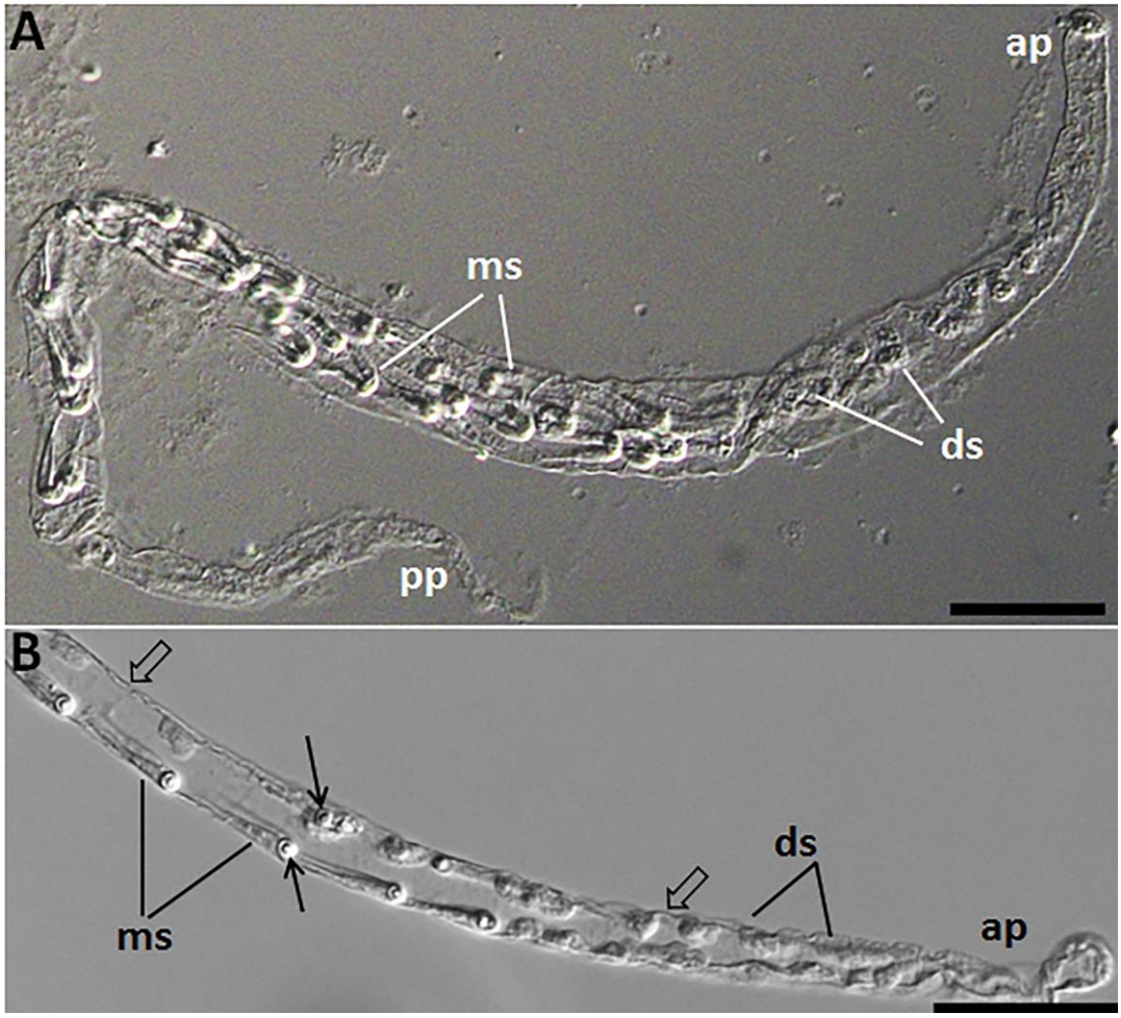

699

700 Figure 7: Differential interference contrast (DIC) photomicrograph of plasmodia of
701 *Ceratomyxa vermiformis* sp. n. from the gallbladder of *Colossoma macropomum*. A
702 and B: vermiform-shaped plasmodia showing developmental stages (ds) in the
703 anterior pole (ap) and mature myxospores (ms) in the middle and posterior pole
704 (pp). In B note mature spores (ms) and the sporogonic developmental stages (ds)
705 are closely associated with the external layer (black arrows). Polar capsules (white
706 arrows). Scale bars = 40 μm.
707
708

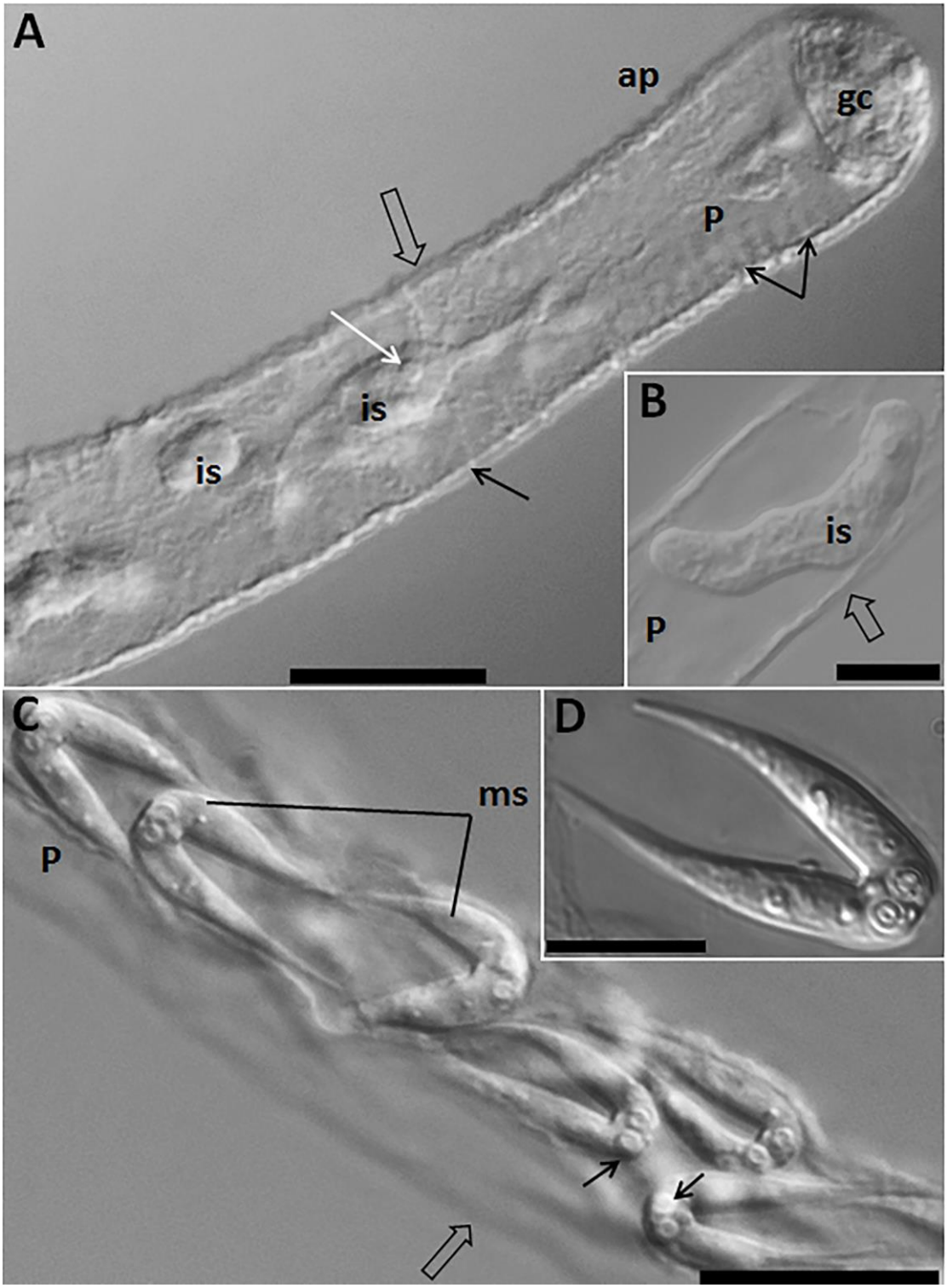

Figure 8: Differential interference contrast (DIC) photomicrograph showing details of plasmodia and spores *Ceratomyxa vermiformis* sp. n. from the gallbladder of *Colossoma macropomum*. A: anterior pole (ap) of a plasmodium (P) showing the growth centre (gc), wall (black thick arrow) and immature spores (is). Note transverse corrugations (black thin arrows) and the polar capsules (white thin arrow). Scale bar = 20 µm. B: early developmental spore stage near the external layer (large arrow) of the plasmodium (P). Scale bar = 10 µm. C: mature spores

(ms) inside of the plasmodium (P) with thick arrow showing wall and thin arrows showing polar capsules. Scale bar = 20 µm. D: mature spore. Scale bar = 10 µm.

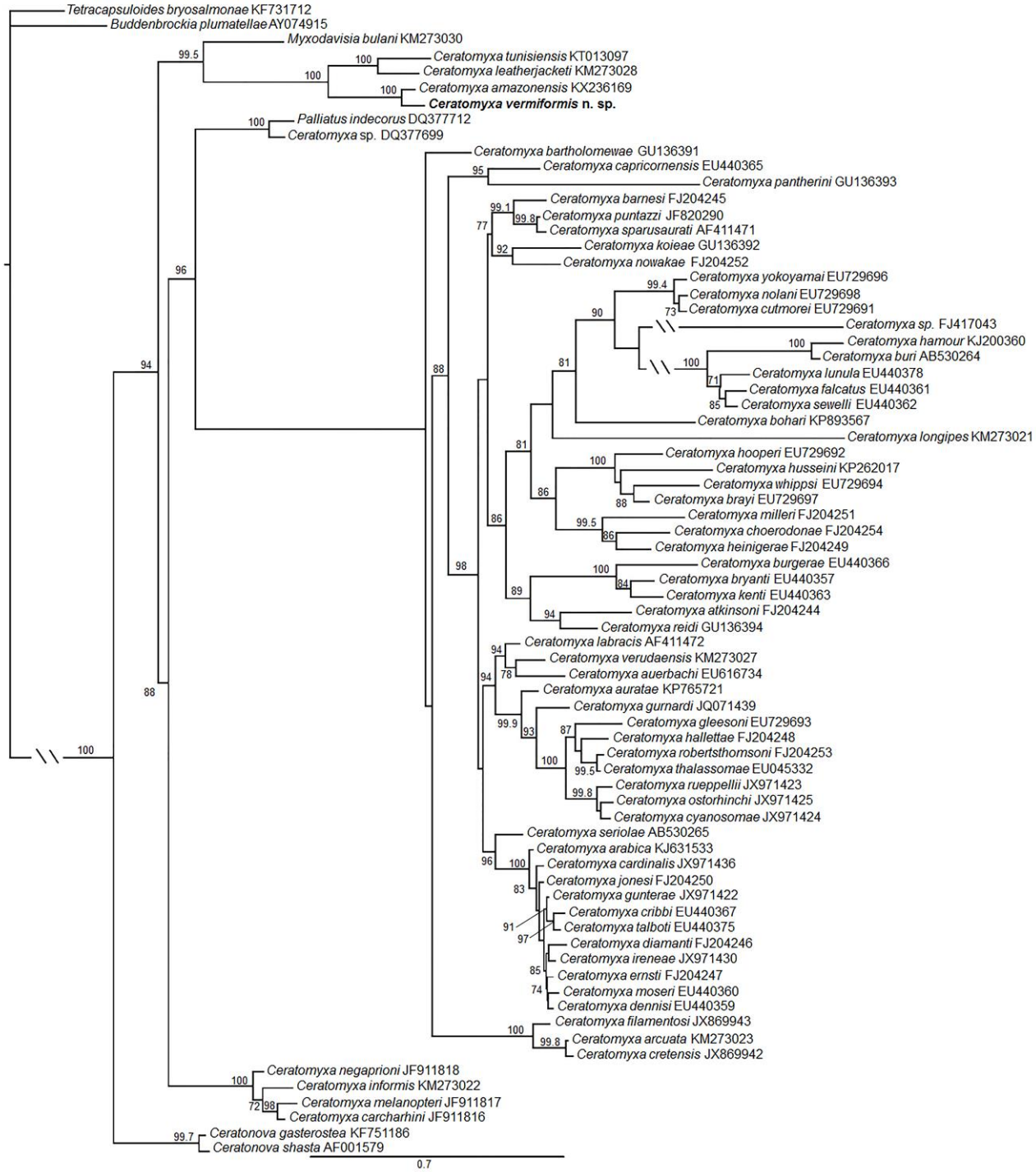

Figure 9: Molecular phylogenetic tree based on maximum likelihood analysis of SSU rDNA showing the position of *Ceratomyxa vermiformis* sp. n. parasite of gallbladder of *Colossoma macropomum*. Bootstrap values above 70 are indicated at the nodes. GenBank accession numbers after the species name.

Supplementary Figures

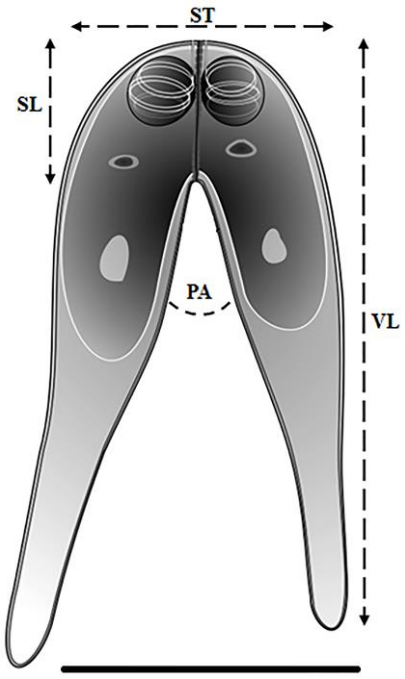

Figure S1: Schematic representation of a mature spore of *Ceratomyxa vermiformis* sp. n. from gallbladder of *Colossoma macropomum* and details of how the measurements were made. Scale bar = 10 µm. SL = spore length; ST = spore thickness; VL = valve length; PA = posterior angle. Spore width was measured perpendicular to and at the midpoint of spore thickness.

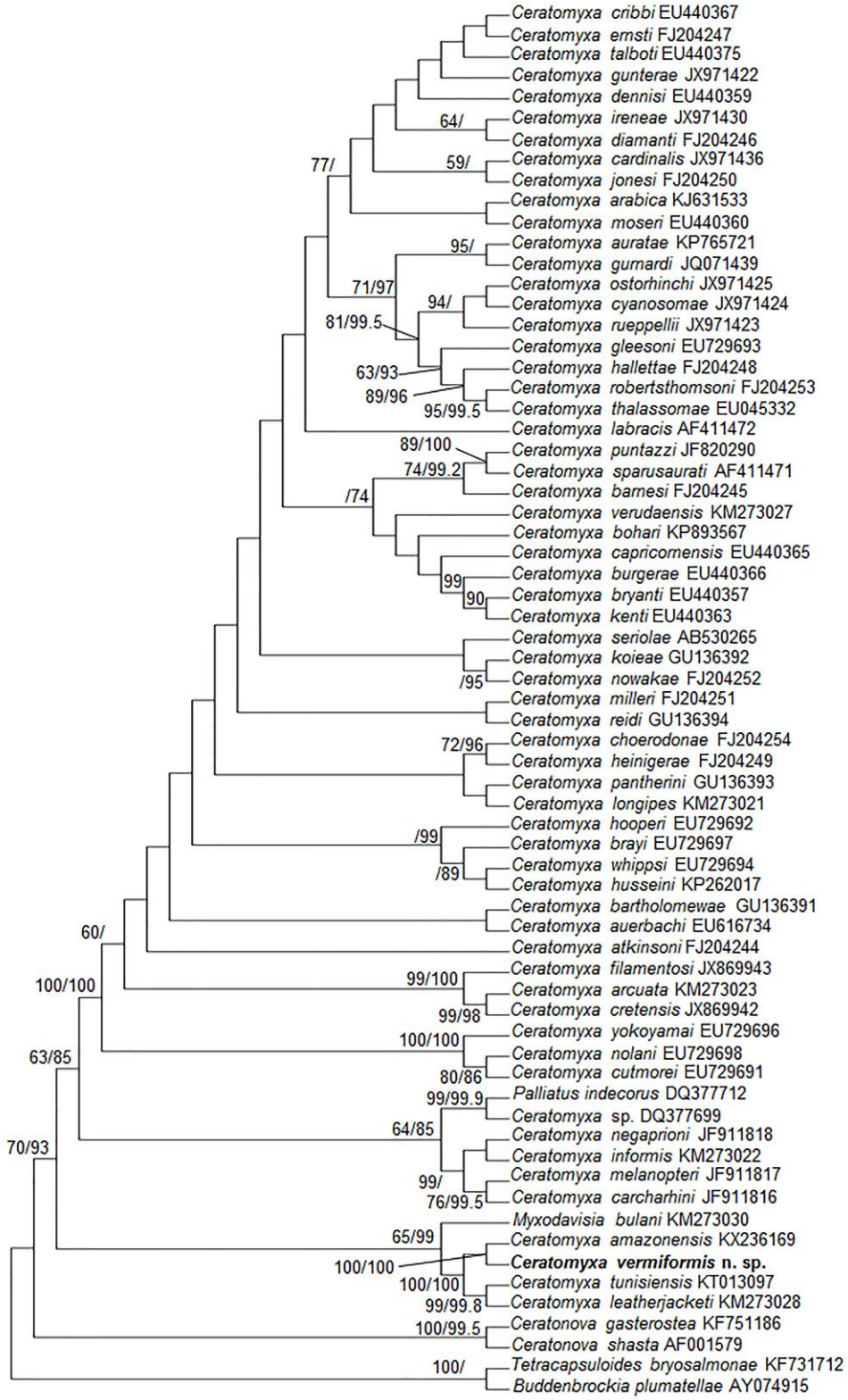

Figure S2: Maximum parsimony tree showing relationships of *Ceratomyxa vermiformis* sp. n. from gallbladder of *Colossoma macropomum* based on partial SSU rDNA. Bootstrap values above 50 in maximum parsimony (MP) and maximum likelihood (ML) analyses are indicated at the nodes as MP/ML. GenBank accession numbers after the species name.

785 Table 1 – Sites and periods of collection of *Colossoma macropomum* in the Amazon Basin, the number of fish examined, their sizes (total
786 length), and the number parasited by *Ceratomyxa vermiformis* sp. n. Most fish were immature (≤ 55 cm; Costa *et al.* 2001). Size ranges
787 are provided when relevant for distinguishing immature and mature fish.

Locality	Latitude/longitude	Period of collection	No. fish examined	Fish size (and n-value)	No. fish infected (and prevalence)
Tapajós River, Santarém/Pará State.	02º 20`03.46``S; 54º52`33.86``W	October 2014	10	29-42 cm (7); 62- 69 cm (3)	5 (50%)
		March 2015	18	16 – 53 cm	0
		January 2016	8	23-30 cm (5); 69-74 cm (3)	0
Amazon River, Laranjal do Jari/Amapá State	01º08`17.24``S; 51º48`31.94``W	September 2015	1	29 cm	1 (100%)
Solimões River, Manacapuru/Amazonas State	03º03`46.49``S; 61º09`29.91``W	December 2015	16	28-40 cm	0

788

789

Table S1. Comparisons of dimensions (in µm) of the spores of *Meglitschia mylei* and *Ceratomyxa vermiformis* n. sp. from the Amazon basin.

Species	SL	LA	SW	ST	PC	PFt	Host
M. mylei	24.6±0.8	20.1±0.7	8.7±0.4	5.1±0.3	2.1±0.3	5-6	*Myleus rubripinnis*
C. vermiformis* n. sp.	25.6±2 (22–29)	>18.8±0.7 (17.6–19,3) >17.5±08 (16.4–18.3)	8.4±0.4 (7.9–9,3)	5.4±03 (4.9 – 5.7)	2.7 ± 0.1	3-4	*Colossoma macropomum*

	SL	LV	SW	ST	PA
C. vermiformis* n. sp.*	4.5±0.2 (4.8–4.2)	>23.7±0.7 (22.1–24,3) >21.9±08 (20.6–23)	5.4±03 (4.9 – 5.7)	8.4±0.4 (7.9-9.3)	30.2±6.6º (22–43º)

*Measured obtained in accord to those of Azevedo et al. (2011) to *M. mylei* for effect of comparison. **Measured obtained as those of *Ceratomyxa* species in accord to Gunter et al. (2009). SL: length; LA: length appendices; LV: length valves; SW: width, ST: thickness; PCs: Polar Capsule diameter; PFt: Polar filament turns; PA: Posterior angle.